ORIGINAL RESEARCH   **Open Access**

A new two-degree of freedom combined PID controller for automatic generation control of a wind integrated interconnected power system

Appala Naidu Karanam* and Binod Shaw

Abstract

Frequency control of an interconnected power system in the presence of wind integration is complex since wind speed/power variations also affect system frequency in addition to load perturbations. Therefore, improving existing control schemes is necessary to maintain a stable frequency in such complex power system scenarios. In this paper, a new 2-degree of freedom combined proportional-integral and derivative control scheme is applied to a wind integrated interconnected power system. In designing the controller, several inputs used for a secondary frequency control loop are considered along with the merits of the existing controllers. The combined controller provides better control action than existing controllers in the presence of wind as is evidenced by the wide variety of results presented. For tuning of the controller gains, a crow search optimization algorithm (CRSOA) is used. Results are obtained via the MATLAB/Simulink software.

Keywords: Load frequency control, 2-DOF-PID controller, Crow search optimization algorithm

1 Introduction

Power imbalance between generating and demand units is the main reason for frequency deviation, while the integration of renewable resources into a power network increases the imbalance which in turn influences system frequency. Scrutiny of stability in interconnected power systems is a significant issue because of the advanced nature and complexity of the modern power system. A slight discrepancy in the real power demand and its associated losses from active power generation can deviate the operating frequency and tie line power from their nominal values [1]. Primary control can be achieved by appropriate selection of speed regulation parameter 'R', while an ancillary service like Automatic Generation Control (AGC) addresses the problem due to both

frequency and tie line power deviations by nullifying the area control error (ACE) and conserving system stability in addition to engaging the security and reliability constraints in the system [2]. The key intentions of AGC are to enhance the dynamic response of the system by damping the steady state frequency and to keep power exchange deviations within tolerable limits. It alters the operating points of the generators to harmonize with the continuously changing load demand, as advocated by an appropriate control strategy. Integration of renewable energy sources like photovoltaics (PV), wind turbines, energy storage systems, fuel cells (FC) and batteries with conventional power system is expanding because of generation shortfall and depletion of fossil fuels, increasing fuel cost, environmental concerns and global warming. However, they add a burden to the control strategy because of their limitations [3–5]. Classical AGC controllers have proven to be robust and are well suited for decentralized systems when the system parameters

*Correspondence: karanam2010@gmail.com
Department of Electrical Engineering, National Institute of Technology, Raipur, India

are rigid. Classical controllers of I, PI, ID, PID, IID, and PIDN have been extensively used and covered in the literature because of their simple mathematical models and practical feasibility [6], though they have been found to be burdensome in assuring stability in the non-linear AGC problem. The superiority of a controller depends on not only its fast control action but also its ability to sustain the nonlinearities such as governor dead band (GDB) and boiler dynamics (BD). Cascading the independent classical controllers facilitates more options to attenuate the disturbance and process the error accurately to simulate a smooth transient response. PI-PD [7] and PD-PID [8, 8] are used in AGC to test their capability for wide variations in load and system parameters. The flexibility and robustness of supplementary control in an AGC can be enhanced by incorporating higher degrees of freedom. A 2-DOF-PID controller has one additional closed loop transfer function that can be independently controlled to track the set point and reject noise. The empirical formulae for optimal parameters and its functions are given in [10]. The optimized 2-DOF-PID and 2-DOF-IDD controllers are implemented successfully in AGC and this leads to significant reductions in the performance index [11–13]. A 2-DOF-FOPID is implemented for three unequal thermal power systems with GRC and it provides good time response characteristics under load uncertainties [14, 14]. However, there is a compromise among the inversely related disturbance and noise rejection parametrics.

The aforementioned shortcomings motivate the design of a combined controller. Based on the merits of 2-DOF-PID controller with filter coefficient and regular PID controller without filter, they are recombined to produce improved control for a plant. Optimization algorithms enhance the effectiveness of the controllers by apposite selection of tuning parameters and nullifying ACE swiftly, thereby aiding the suitability and selectivity of the controller. The Crow search optimization algorithm [16] is demonstrated to be a better tuner than existing optimization techniques [5]. In this paper, the effectiveness of the combined controller is exhibited by optimizing the gains using the crow search algorithm for superior dynamic response of the system and to yield better performance than existing controllers. The combined controller performance is tested on a multi-area interconnected system without wind integration, with wind integration, load perturbations, and wind changes along with noise. The detailed illustrations regarding the structure of the controller, optimization algorithm and results are presented in the following sections.

2 System studied

In this paper, a two-area interconnected power system with wind penetration and thermal units in individual areas is simulated in MATLAB/Simulink to investigate the new combined controller scheme. Figure 1 shows the simulated system block diagram, in which area I consists of one thermal plant integrated with sufficient wind generation whereas area II is operated with a single thermal
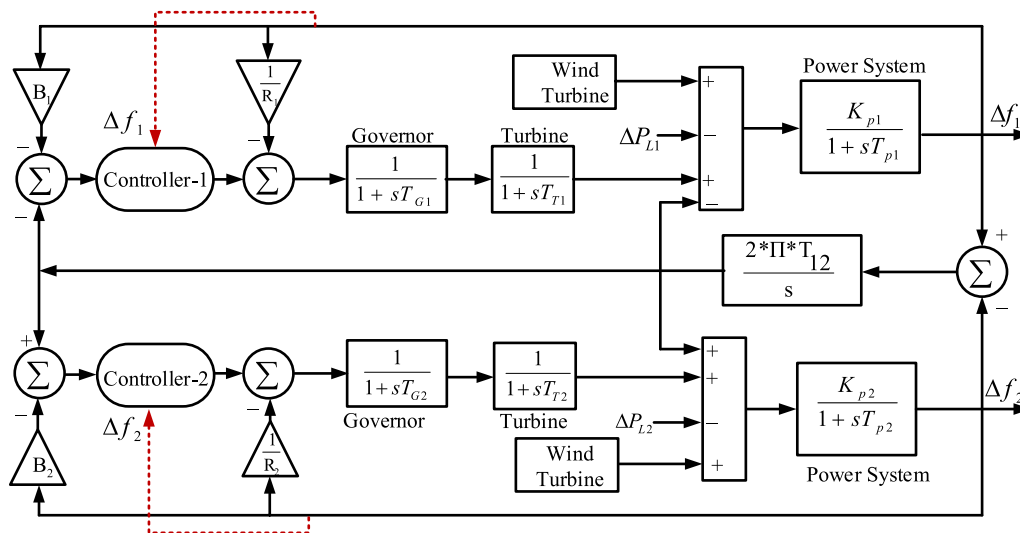

Fig. 1 Schematic Block diagram of two area interconnected system with wind integration

plant. Investigations are carried out in three cases to show the improvement in the stability of the interconnected power system in the presence of the combined controller in two scenarios of wind integration. In case 1, load perturbations are considered in a particular area where the wind power is maintained at a constant level. In case 2, limited variation in wind speed is considered along with regular load changes but the overall contribution of the wind change is less than the demand variation and therefore has limited influence on the system frequency. Large wind variations are introduced along with load changes in case 3. In all these cases, wind changes do not dominate load perturbations and hence the additional frequency oscillations caused by these changes are negligible. However, the wind speed/power changes in area I dominate load perturbations and severe frequency oscillations are observed. Hence, suitable controller design is essential to minimize the frequency disturbances caused by load and wind power variations. The load perturbations are simulated with step functions and the wind power generation is designed with a stochastic model available in [17, 17]. Under these disturbance models, the system response is studied using the combined controller and is compared with existing PID and 2-DOF-PID controllers. The performance of the combined controller is evaluated in two scenarios and the structure of the controller and its mechanism are provided in Sect. 3.

3 Combined 2 DOF PID coupled classical controller

Several controllers have been applied to the AGC problem to maintain the system frequency within limits during load disturbances. During random load perturbations, the presence of a PID controller in the generation secondary control loop of multi-area interconnected power systems provides better performance than either with an I/PI controller or without a controller. Because of the integration of renewable sources, additional disturbances are added to the AGC problem and hence a proper control strategy is needed in order to limit frequency oscillations for such additional disturbances along with load changes. Therefore, a new proposed controller is investigated for wind integrated power systems. A classical PID without filter-coefficient and a 2-DOF-PID controller with filter coefficient are chosen for implementation of the combined complex controller to satisfy control system performance specifications and to provide superior results. Figure 2 shows the 2-DOF-PID-controller connection structure for plant $P(S)$, one which utilizes two inputs called reference input $R(S)$ and output $Y(S)$. To improve the response of the control system under large and regular disturbances, an additional PID controller $C_2(S)$ is connected with the help of output signal $Y(S)$ along with original control blocks of the 2-DOF-PID controller $F(S)$ *and* $C_1(S)$. This modified combined controller set up for the plant is shown in Fig. 3, and the
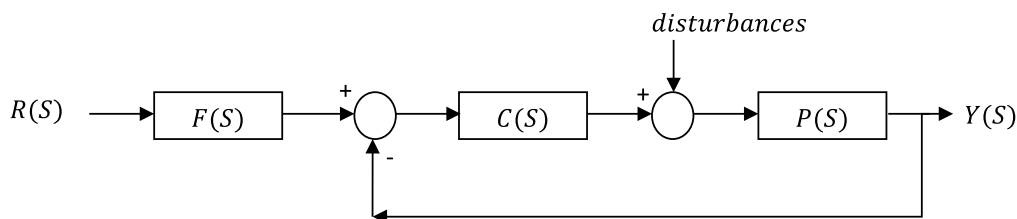

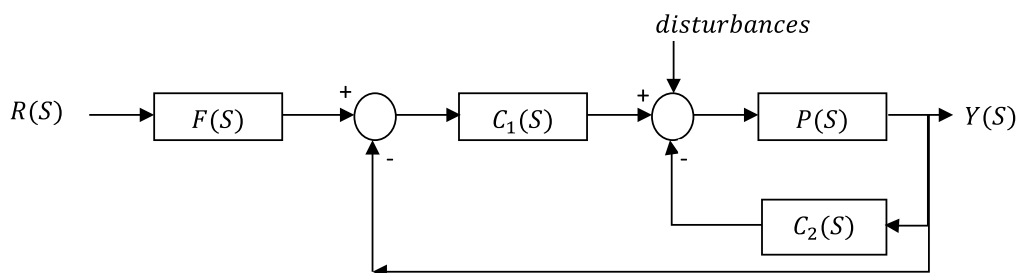**Fig. 2** Controller structure of 2-DOF PID controller

Fig. 3 Controller structure of combined controller

transfer functions of the combined individual controller components are given by:

$$F(S) = \frac{(P_w k_p + D_w k_d)S^2 + (P_w k_p N + k_i)S + k_i N}{(k_p + k_d N)S^2 + (k_p N + k_i)S + k_i N} \tag{1}$$

$$C_1(S) = \frac{(k_p + k_d N)S^2 + (k_p N + k_i)S + k_i N}{S(S + N)} \tag{2}$$

$$C_2(S) = \frac{k_{dc}S^2 + k_{pc}S + k_{ic}}{S} \tag{3}$$

In (1), P_w and D_w are the weighted coefficients of degree of freedom controllers, N. is the first order filter coefficient, k_p, k_i and k_d. are the proportional, integral, and derivative parameter gains of the 2-DOF-PID controller, respectively. In (3), k_{pc}, k_{ic} and k_{dc} are the proportional, integral, and derivativearameter gains of the coupled PID controller, respectively. The proposed contller structure shown in Fig. 3 has an additional feedback control block $C_2(S)$ to provide additional stability and fast response since its structure is a regular PID controller. On the second side, there is no additional input requirement for the combined controller as it uses the same reference input $R(S)$ and output $Y(S)$ as the 2-DOF-PID controller. Together, the control input to the plant from the combined controller is given by:

$$U(S) = F(S).C_1(S).R(S) - (C_1(S) + C_2(S)).Y(S) \tag{4}$$

In (4), the additional control signal provided with the help of two control blocks of the combined controller set up with output signal as input is capable of decreasing additional oscillations and increases the overall stability of the system. The effect of this additional controller is presented in detail in Sect. 5.

4 Application of controllers to the LFC problem with tuning mechanism

Since the control signal provided by most of the advanced secondary controllers to reduce the frequency oscillations of the power plant uses two-reference input signals, known as ACE and change in frequency Δf. A regular PID controller uses the ACE signal as reference in a multi-area interconnected power system scenario and change in frequency in the isolated scenario. As both signals are available in each area, the PID component in the combined controller is actuated by Δf instead of the ACE signal. This eliminates the additional noise at corner points in the LFC problem and complications in practical
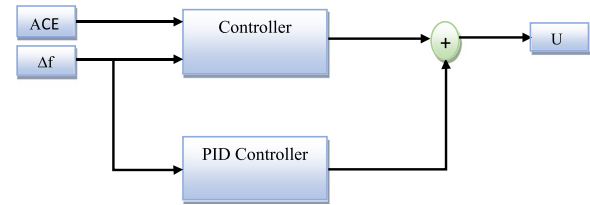

Fig. 4 Block diagram controller structure of combined controller in ALFC application

applications. The combined secondary controller set up for minimization of frequency oscillations of interconnected power system scenario is presented in Fig. 4.

The combination of two controllers increases the number of decision variables to 9 and hence a centralized controller structure is opted for here, so that even though the number of plants of each area increases the dimension of the control problem remains the same. For optimal tuning of these combined controller parameters, the crow search optimization algorithm (CRSOA) is adopted. CRSOA is a heuristic population search-based algorithm implemented from crows' intelligence introduced by Askar Zadeh in 2016 [16]. Crows are known as clever birds which interact in all critical situations to achieve better group solutions. After some time period, crows recall their food hiding places and the memory allocations help to achieve better solutions in real time problems. Another interesting fact is that crows can also cheat other crows by moving to another place. By taking these merits of the intelligence in crows, the CRSOA algorithm is proposed. In the CRSOA, assuming that N is flock size and n is the number of decision variables of the problem, the initial solution of the problem (position of each bird at iteration k) is denoted as:

$$X_{i,k} = [x_{i,k}^1, x_{i,k}^2, \ldots, x_{i,k}^n] \tag{5}$$

Since the crows have memory of the food the hiding places are given by (the allocation is different for different crows):

$$M_{i,k} = \left[m_{i,k}^1, m_{i,k}^2, \ldots, m_{i,k}^n \right] \tag{6}$$

Equations (5)–(6) are the steps in initialization of the CRSOA. Based on memory strategies of individual crows, the new position of crow i is obtained as follows:

$$X_{i,k} = X_{i,k} + r_i \times fl_{i,k} \times \left(M_{i,k} - X_{i,k} \right) \tag{7}$$

where r_i is a random number and $fl_{i,k}$ is the flight length. Based on awareness probability (AP), the position of a crow for the next iteration is selected as:
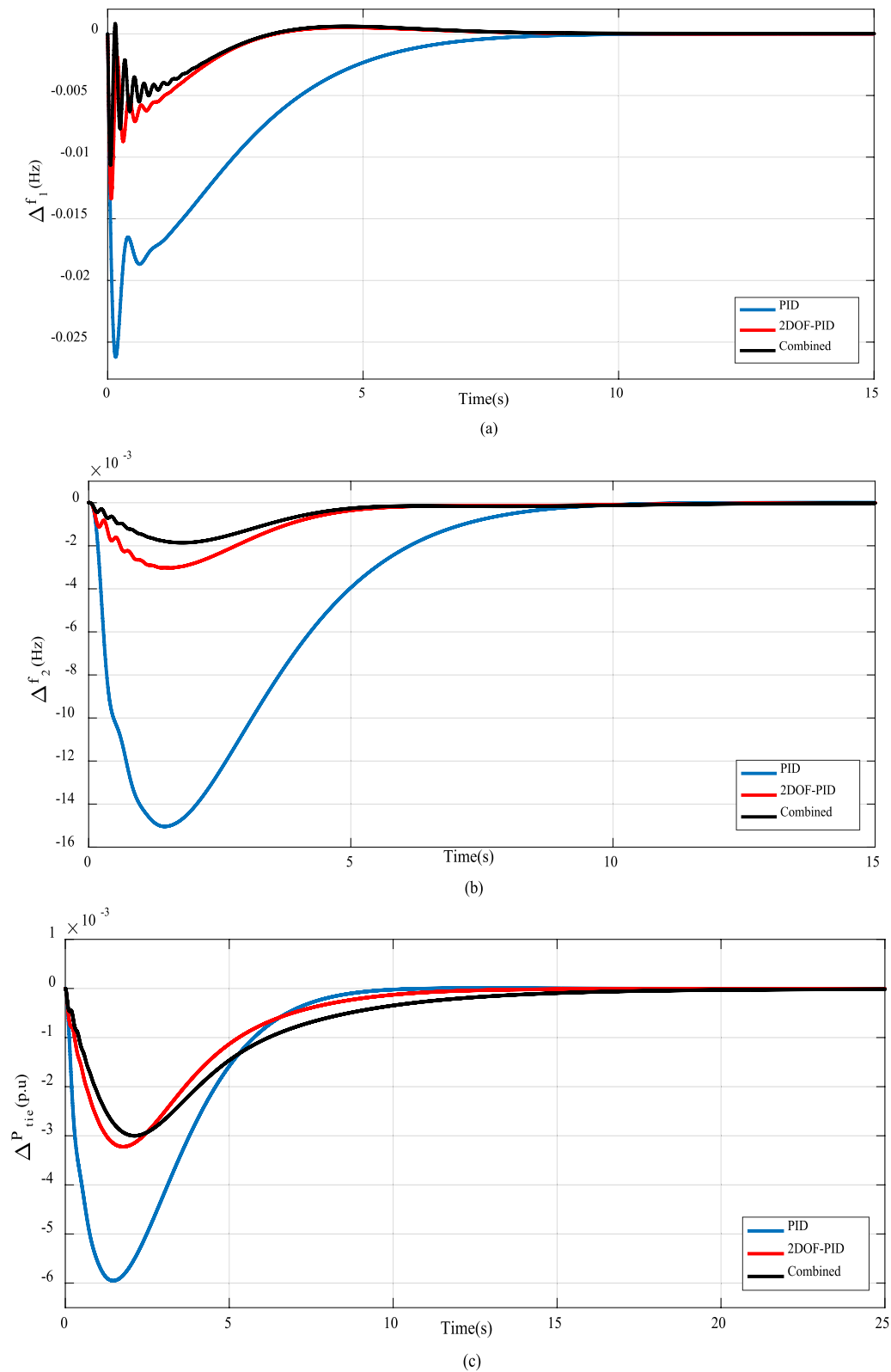
Fig. 5 Improvement in response with the combined controller when the load in area I changes without wind integration. **a** Area 1 frequency change; **b** area 2 frequency change; **c** tie line power change

Table 1 CRSOA tuned controller parameters of the system without wind penetration

Controller parameter	PID controller		2 DOF controller		Combined controller	
	I	II	I	II	I	II
k_p	1.9987	0.8673	1.9963	1.7964	1.9946	1.0805
k_i	1.9857	0.6151	1.4486	1.9095	1.7181	1.5478
k_d	1.9928	1.0057	1.8674	1.5534	1.5704	1.2361
P_w	–	–	1.9998	1.6312	1.7184	1.5921
D_w	–	–	1.7804	1.0357	1.0858	1.7259
N	–	–	173.23	142.13	180.22	173.64
k_{pc}	–	–	–	–	1.7871	1.0889
k_{ic}	–	–	–	–	1.9328	1.5429
k_{dc}	–	–	–	–	1.8226	1.2258

Table 2 CRSOA tuned controller parameters of the system with wind penetration

Controller parameter	PID controller		2 DOF controller		Combined controller	
	I	II	I	II	I	II
k_p	1.9867	1.9791	1.9852	1.8389	1.9861	1.5568
k_i	1.1271	1.0157	1.8334	1.2309	1.4895	1.4736
k_d	1.9896	1.9752	1.7548	1.8128	1.7331	1.4837
P_w	–	–	1.9942	1.0276	1.7155	1.4044
D_w	–	–	1.7532	1.7395	1.8975	1.5054
N	–	–	199.86	116.26	126.50	142.81
k_{pc}	–	–	–	–	1.5246	1.2939
k_{ic}	–	–	–	–	1.8517	1.3978
k_{dc}	–	–	–	–	1.6330	1.3517

Table 3 Comparison of performance specifications during load perturbation in presence of wind noise

	Δf_1			Δf_2		
	PID	2 DOF PID	Combined	PID	2 DOF PID	Combined
Peak change (Hz)	− 0.0522	− 0.0266	− 0.0213	− 0.0283	− 0.0058	− 0.0035
Setting time (s)	12	10	10	12	08	06
Steady state error (Hz)	2.5×10^{-4}	1.4×10^{-4}	1.2×10^{-4}	1.9×10^{-4}	-0.1×10^{-4}	0.3×10^{-4}

Table 4 Comparison of performance specifications during increasing mode of wind penetration

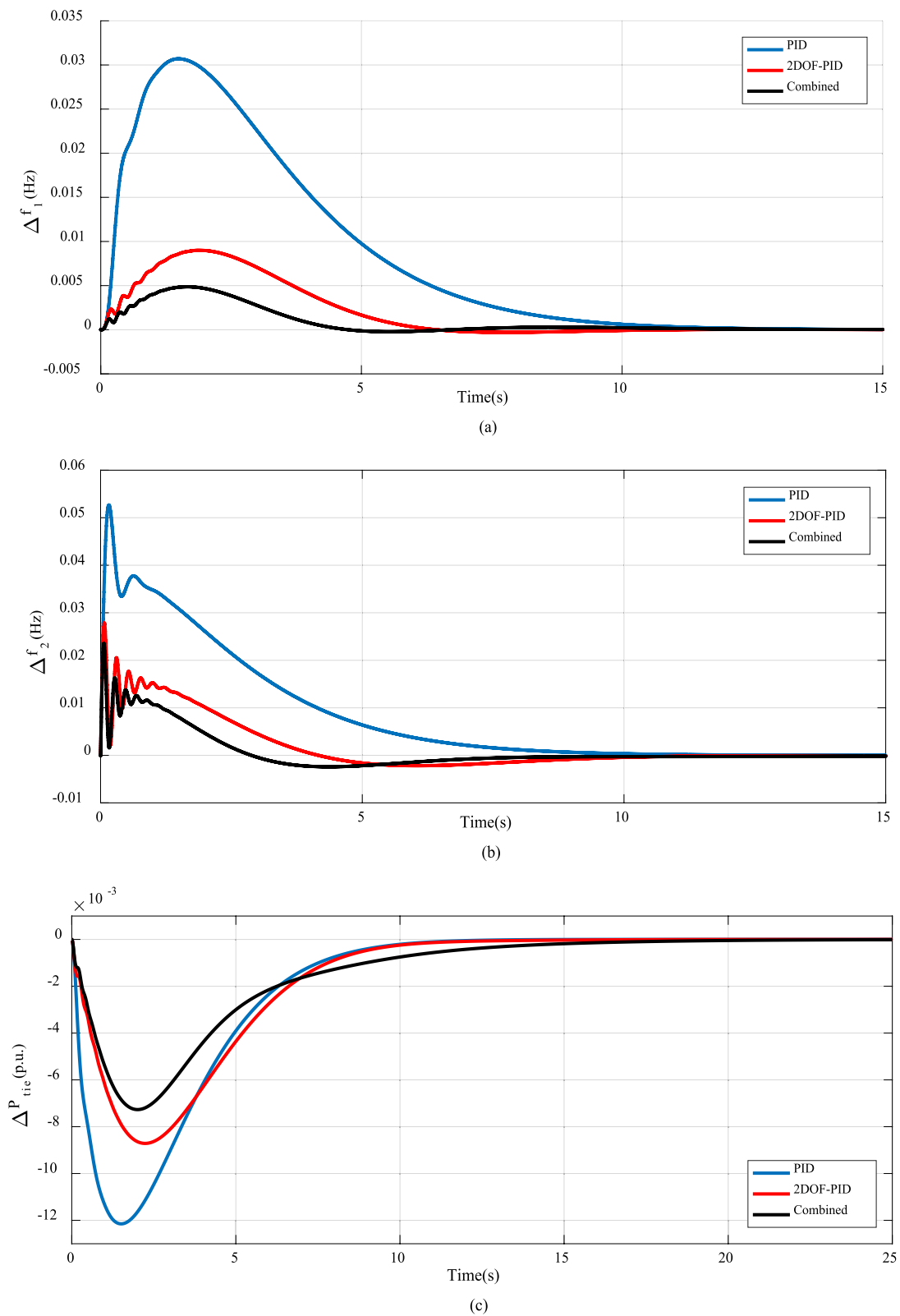|	Δf_1			Δf_2		
	PID	2 DOF PID	Combined	PID	2 DOF PID	Combined
Peak change (Hz)	0.0069	0.0021	0.0016	0.0065	0.0012	0.0008
Setting time (s)	14	07	05	14	08	06
Steady state error (Hz)	1.0×10^{-4}	0.5×10^{-4}	0.2×10^{-4}	6.5×10^{-4}	2.1×10^{-4}	1.8×10^{-4}

Fig. 6 Improvement in responses when the load in area 2 changes without wind integration. **a** Area I frequency change; **b** Area II frequency change; **c** Tie line power change
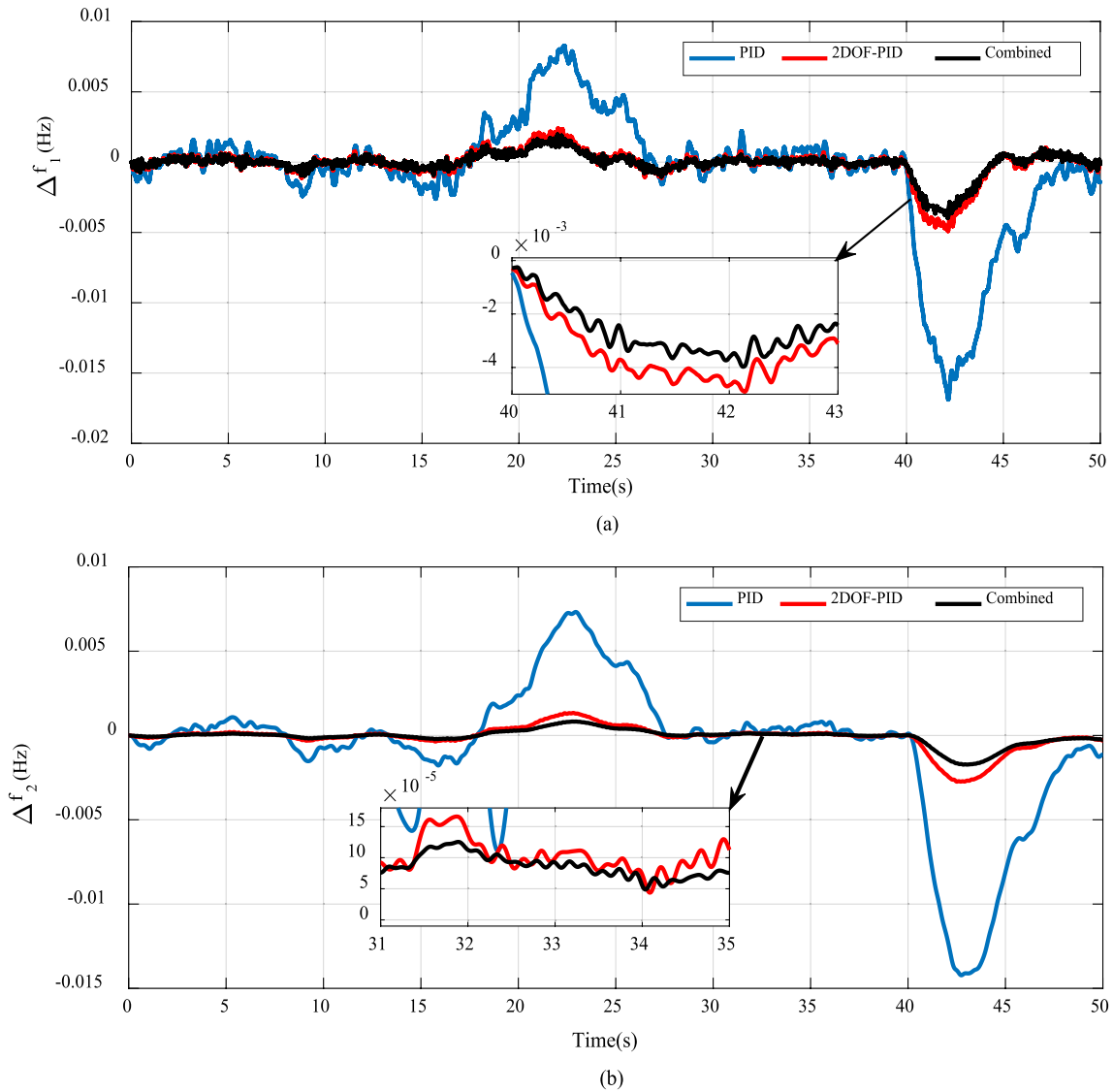
Fig. 7 Frequency disturbances generated during wind variations with secondary controllers (wind power variation in area I with 3% increase at 20 s and 6% decrease at 40 s without SLP). **a** Area I; **b** area II

$$X_{i,k+1} = \begin{cases} X_{i,k} + r_i \times fl_{i,k} \times (M_{i,k} - X_{i,k}) & r_i \geq AP \\ \text{random} & \text{otherwise} \end{cases}$$

(8)

Depending on AP values, the CRSOA changes its search region and r_i is a uniform distribution between 0 and 1. The intelligent behavior of crows inculcated in the algorithm provides global optimum solutions. For identification of optimal values of the combined controller, ones which minimize the overall frequency oscillations of each area in the interconnected power system, an objective function is framed with the output variables and the value of the objective function depends on the controller parameter selection. Since the test system consists of two areas with three output variables known as frequency change in area I (Δf_1), frequency change in area II (Δf_2) and power transfer between the two areas (ΔP_{12}), it leads to a unique fitness function given by:

$$J = \int_0^t ((\Delta f_1)^2 + (\Delta f_2)^2 + (\Delta P_{12})^2) dt$$

(9)

The individual output variables of the system depend on the controller variables and can be decided directly by
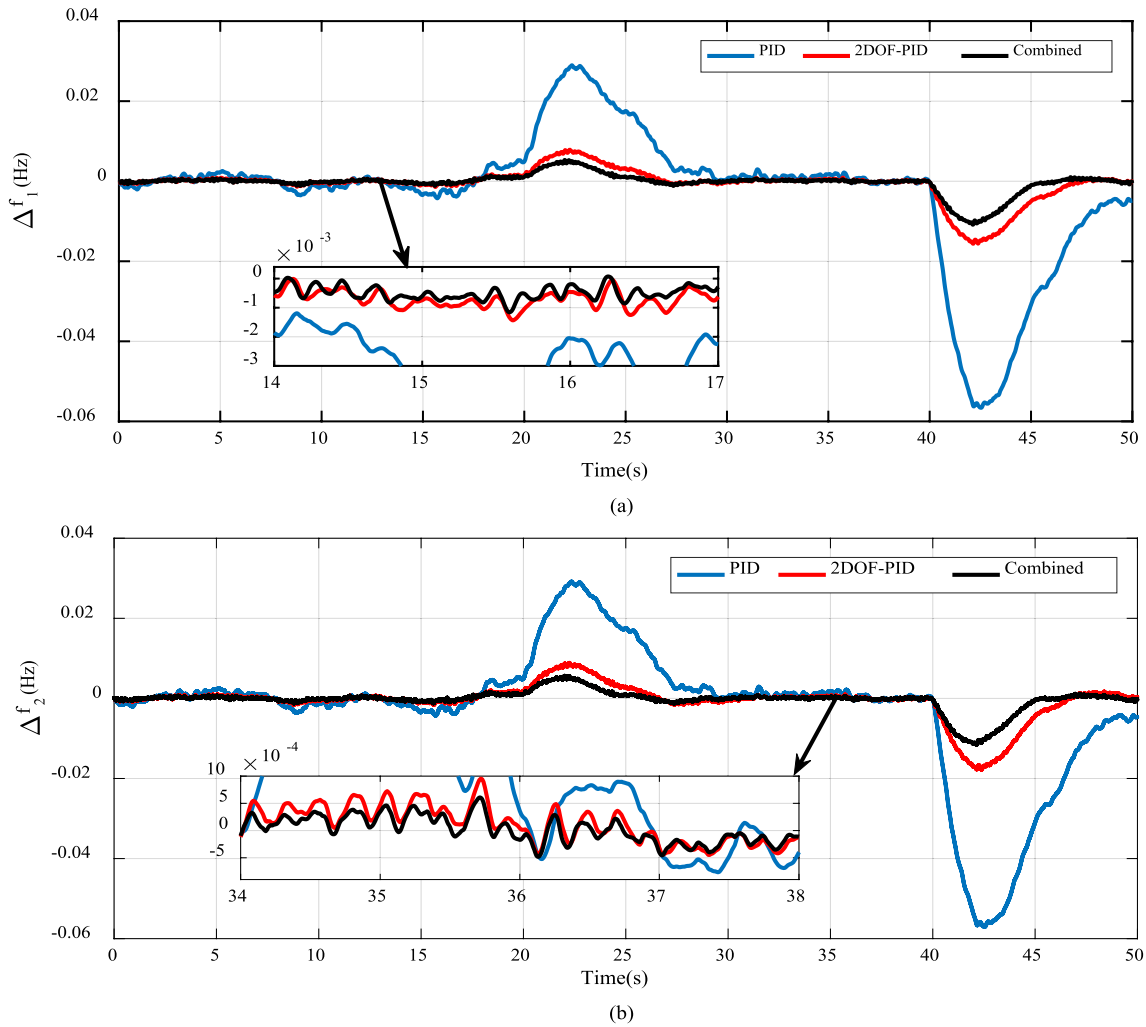
Fig. 8 Frequency disturbances generated with secondary controllers when both areas are equipped with wind penetration (wind power variation in both area I and area II with 6% increase at 20 s and 12% decrease at 40 s without SLP). **a** Area I; **b** area II

the CRSOA. Since the proposed controller is a combination of 2-DOF and PID controllers, a total of 9 variables are required in each area with isolated plants so that the problem dimension is 18 for the two-area interconnected system and the limits of the variables are given by:

$$k_{pminc1} \leq k_{pc1} \leq k_{pmaxc1}$$
$$k_{iminc1} \leq k_{ic1} \leq k_{imaxc1}$$
$$k_{dminc1} \leq k_{dc1} \leq k_{dmaxc1}$$
$$P_{wminc1} \leq P_{wc1} \leq P_{wmaxc1}$$
$$D_{wminc1} \leq D_{wc1} \leq D_{wmaxc1} \quad (10)$$
$$N_{minc1} \leq N_{c1} \leq N_{maxc1}$$
$$k_{pminc2} \leq k_{pc2} \leq k_{pmaxc2}$$
$$k_{iminc2} \leq k_{ic2} \leq k_{imaxc2}$$
$$k_{dminc2} \leq k_{dc2} \leq k_{dmaxc2}$$

In (10), suffix c_1 and c_2 represent the parameters in controller components C_1 and C_2, respectively. However, the same CRSOA is used for tuning the controller parameters of individual 2-DOF and PID controllers for comparison purposes and to show the superiority of the combined controller from different perspectives. All the advantages of the combined controller in different operational modes are discussed in detail in Sect. 5.

5 Simulation results

During small load perturbations, primary regulation of the conventional generating units is capable of maintaining the system in a stable operating region. However, the stability of the system is enhanced with the help of a secondary control mechanism which also provides additional control during large load disturbances to keep the system in that region. Providing proper control becomes
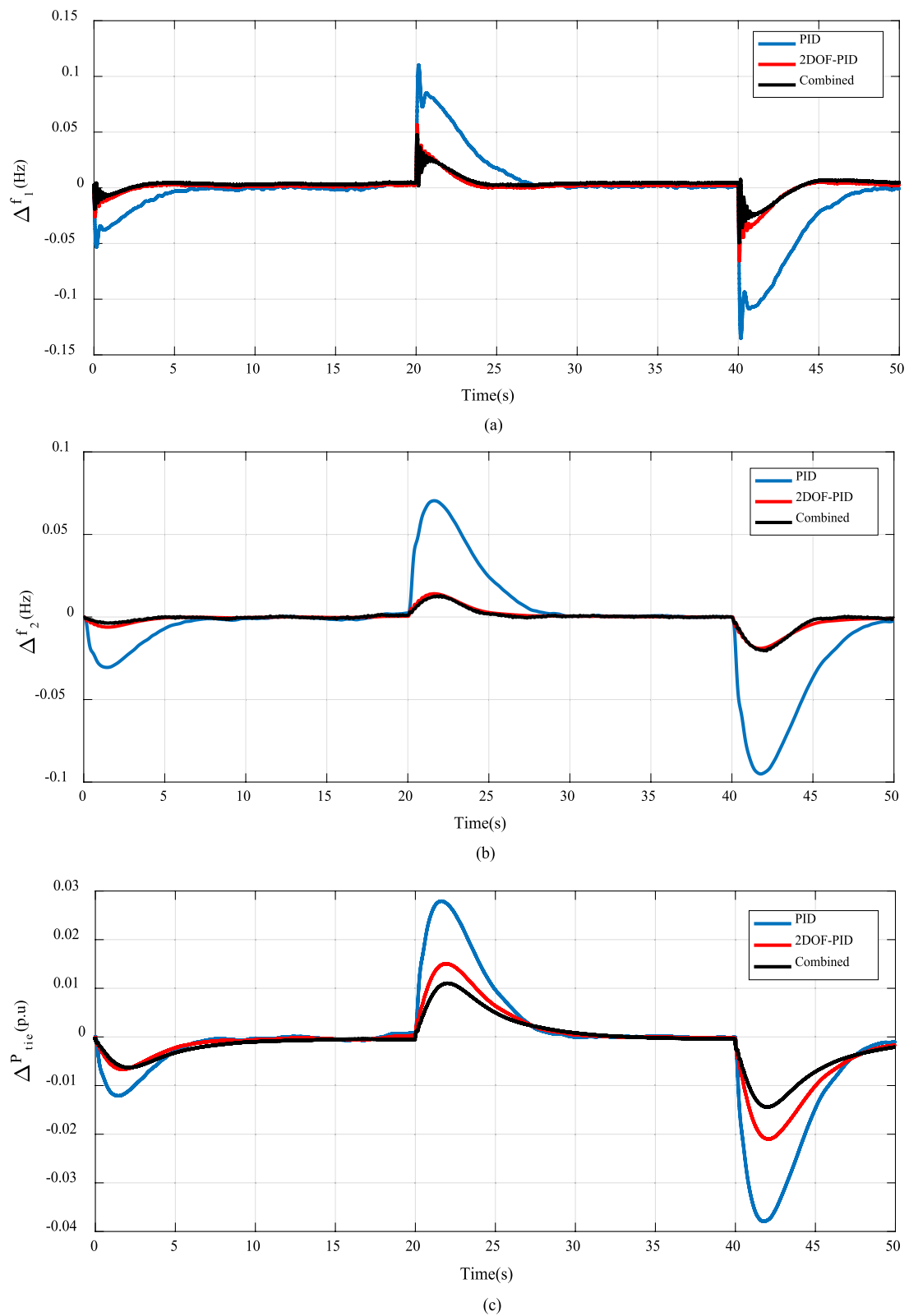
Fig. 9 Improvement in responses with the combined controller during simultaneous changes of load (as shown in Fig. 10), wind disturbances. (+ 3% at 20 s and − 6% at 40 s). **a** Area I frequency change; **b** area II frequency change; **c** tie line power change
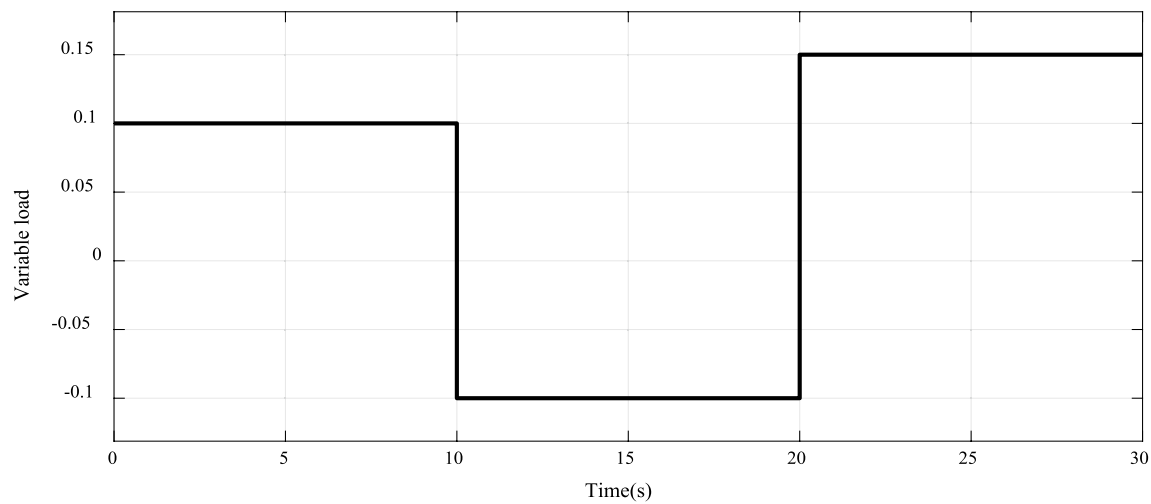
Fig. 10 Variable step load pattern

Table 5 Comparison of performance specifications during decreasing mode of wind penetration

	Δf_1			Δf_2		
	PID	2 DOF PID	Combined	PID	2 DOF PID	Combined
Peak change (Hz)	-0.0142	-0.0042	-0.0033	-0.0132	-0.0021	-0.0012
Setting time (s)	12	07	06	12	08	06
Steady state error (Hz)	-5×10^{-4}	2.5×10^{-4}	2.1×10^{-4}	12×10^{-4}	-2.4×10^{-4}	-2.4×10^{-4}

more complex when the systems are integrated with large wind farms where the wind generation is more volatile in nature. The combined controller is studied here with different wind power along with regular load perturbations, and the results are compared with other controllers.

5.1 Performance of combined controller at constant wind power condition

When the power system is integrated with wind, the relative frequency oscillations are comparatively high because of the particular property of wind speed and power. To study the combined controller in line with the improvements over conventional controllers, initially an interconnected system with constant wind power is considered. This case is similar to a system without wind integration in both areas. In this case, two load perturbation conditions are evaluated and the system outputs are compared to show the efficacy of the combined controller.

When 5% load is decreased in area I at 0 s and the power demand of area II is maintained at a constant level, Fig. 5 shows various output signals of the interconnected power system. Large frequency oscillations are observed

in area I as shown in Fig. 5a since the load disturbances occurred in area I. Because of the interconnection, small frequency changes are observed in area II as shown in Fig. 5b. This happens in the system because of tie line power flow between both areas as shown in Fig. 5c. With this load change, for the traditional interlinked system, the combined controller reduces frequency oscillations of both areas to a greater extent than the other 2 controllers as shown in Fig. 5a, b. The parameters of the combined controller and the existing controller are tuned by the CRSOA with the same common and control parameters. The tuned parameter values are listed in Table 1. In addition to frequency oscillations, the combined controller also reduces the inter tie line power fluctuation during load disturbance. Such improvements are measured in terms of transient and steady state specifications and are presented in Table 3. When the load change condition is reversed, i.e., 10% of load increase in area II at 0 s and the demand of area I is maintained at a constant level, the system responses are presented in Fig. 6. In this case, the combined controller also produces a better response than the existing controllers, and controls the frequency oscillations in a better manner along with tie line power
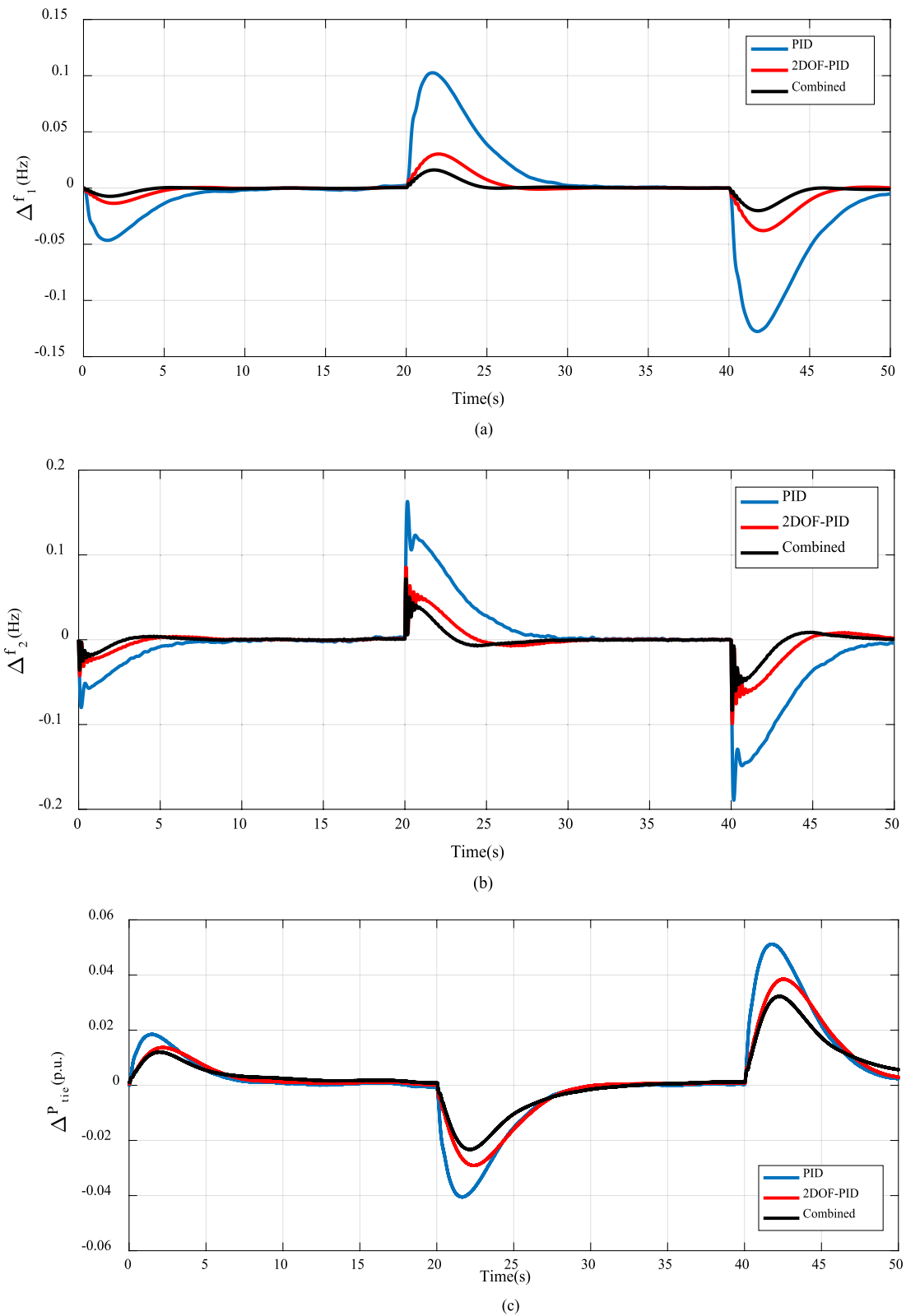
Fig. 11 Improvement in responses with the combined controller during simultaneous load change (as shown in Fig. 12) and wind disturbances (+6% at 20 s and −12% at 40 s). (a): frequency deviations of area I; (b): frequency deviations of area II; (c): tie line power changes
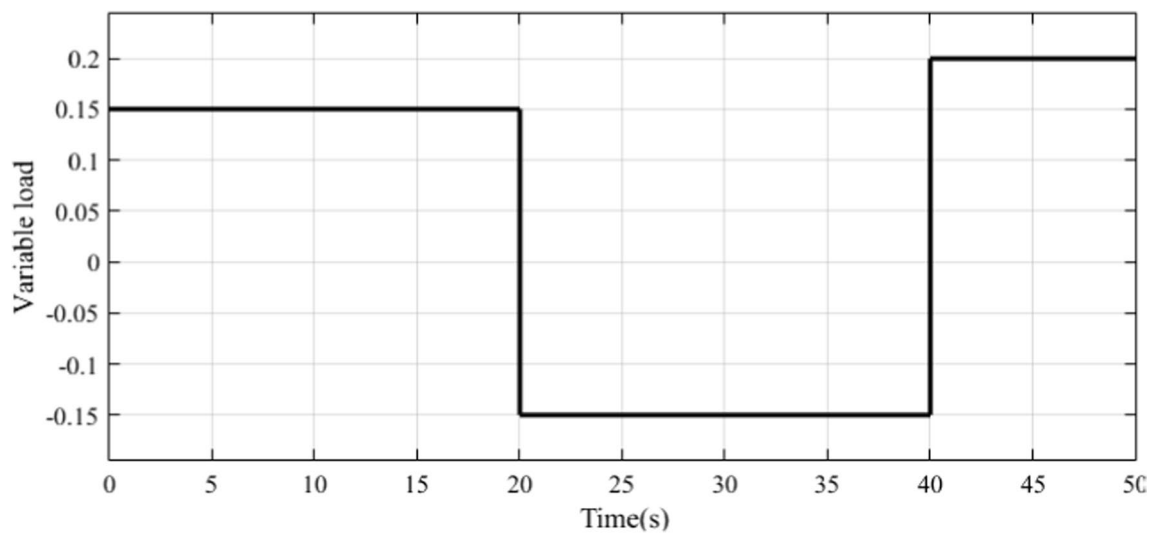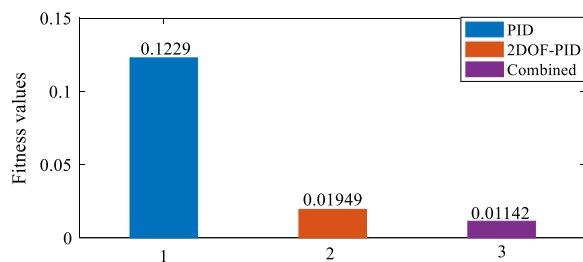
Fig. 12 Variable step load pattern

Fig. 13 Fitness values of the responses with various controllers

fluctuation. The combined controller yields a better solution for minimizing frequency oscillations under any load change in the presence of traditional generating units.

5.2 Performance of combined controller with wind speed noise

When stochastic variations of wind speed are considered, and then are followed by load changes, the responses of PID, 2 DOF and the combined controllers are presented in Fig. 7. The low frequency oscillations caused by small wind variations are reduced by the combined controller in a better manner than with the other two controllers. In both areas, similar observations are obtained. In this case, these variations are inserted in area I only. When both areas are integrated with wind farms and small wind variations are presented during the operation, the responses of the system in the presence of PID, 2 DOF and combined controllers are presented in Fig. 8. In both cases, the combined controller reduces frequency oscillations in a better way than the other controllers irrespective of wind penetration scenarios.

5.3 Performance of combined controller with wind power variations

Along with wind noise and load changes, when wind penetrations in area I change, the performances of the three controllers are presented in Fig. 9. Three types of variations in area 1 are observed in Fig. 9 including wind disturbances of $+3\%$ at 20 s and -6% at 40 s, and load changes as shown in Fig. 10. In the process of minimization of system frequency oscillations, the combined controller provides better control even with wind noise. The control signals provided by the other two controllers are comparatively weak even though all controllers are tuned by the same optimization algorithm. The tuned parameters of PID, 2-DOF PID and the combined controllers are listed in Table 2.

In all the disturbances, the frequency and tie line power oscillations are very low when the combined controller is presented in the secondary control loop of the generating units, and when compared to PID and 2-DOF PID controllers (Table 3). The corresponding performance specifications are listed in Tables 4 and 5 during wind power increase and decrease, respectively. Another important point is that the upper and lower bounds of all the controller parameters are the same when tuned by the crow search algorithm. Major disturbances are initiated in area II and the responses are presented in Fig. 11 with load step changes shown in Fig. 12. In both cases, the combined controller provides the best results.

In addition, fitness values achieved with CRSOA for all three controllers are presented in Fig. 13 for case 1. For the combined controller, the fitness value is 0.01142 which is relatively smaller than the values achieved with PID and the 2 DOF PID controller. The results validate
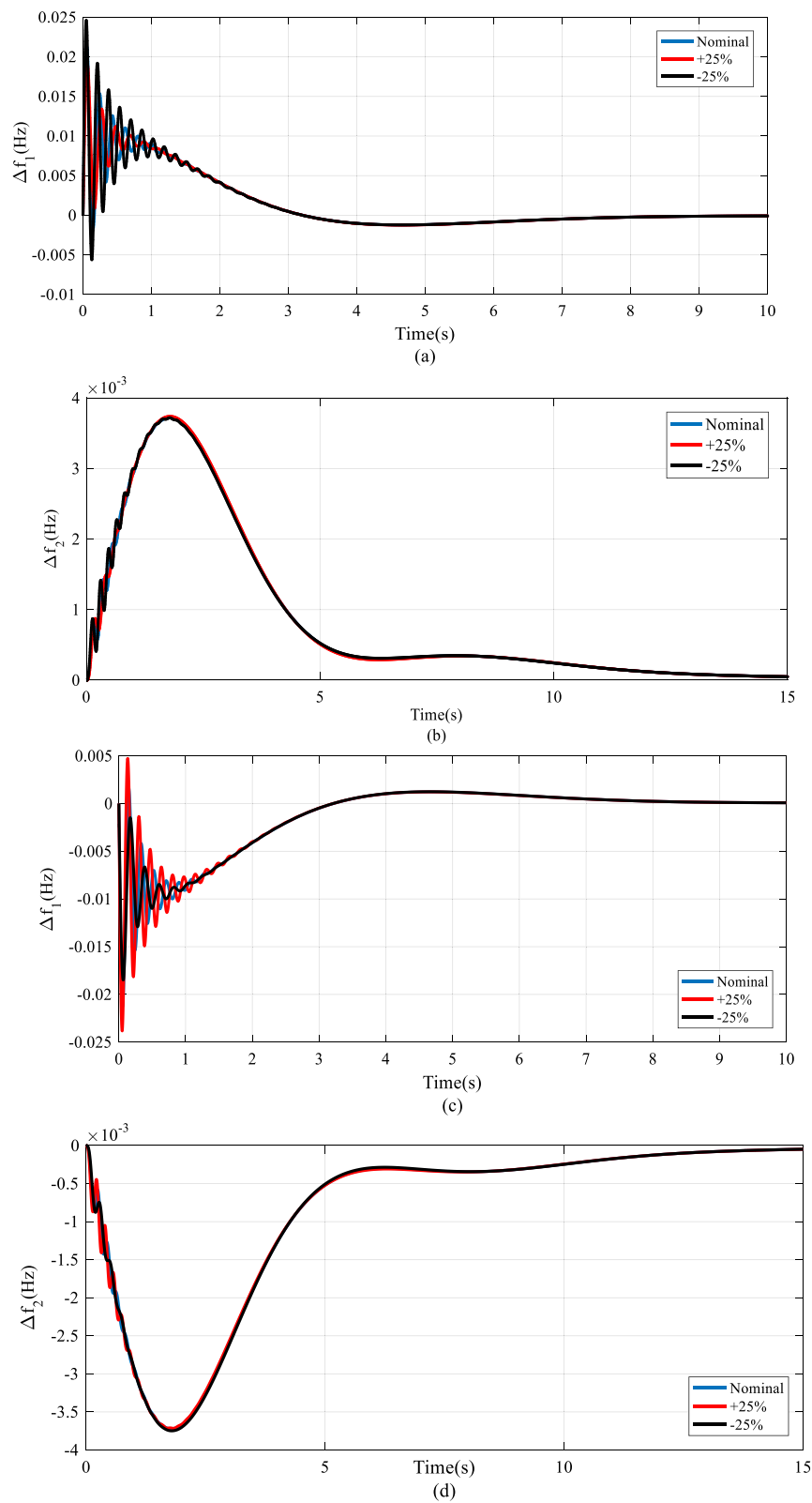
Fig. 14 Influence of system parameter variations on output responses in presence of combined controller. **a** Frequency deviations of area I with variation of K_p; **b** frequency deviations of area II with variation of K_p; **c** frequency deviations of area I with variation of T_p; **d** frequency deviations of area II with variation of T_p

the improvement of response of the combined system during load changes.

5.4 Influence of load and inertia parameter variations on output responses in presence of combined controller

Among all system parameters, the power system gains and time constants vary significantly because of the dynamic nature of the related parameters during operation. When the interconnected power system is equipped with the combined controller in the secondary control loop, the variations of aforementioned parameters are negligible as shown in Fig. 14. Figure 14a, b show the frequency changes of the areas when the power system gain values vary to $+25\%$ and -25%, whereas Fig. 14c, d show the frequency changes of the areas when the power system time constant values vary to $+25\%$ and -25%. From these results, it is very clear that their impact on the output variable values are negligible even for large changes in system parameter values, especially for the combined controller. This shows the advantage of the combined controller over the others in dynamic conditions.

6 Conclusions

Based on the merits of the regular PID and 2-DOF-PID controllers, a new controller is designed to improve the overall response of an interconnected power system in the presence of large wind penetration. The system frequency and inter tie-line power fluctuations are minimized by the combined controller in the presence of continuous load and wind power changes with better performance than existing controllers. This control strategy also reduces parameter variation effects on system outputs, e.g., frequency variation. Overall, the combined controller tuned by the crow search algorithm is the best choice in LFC applications especially with renewable integrated systems for maintaining a stable frequency and power flows.

Appendix

$P_R = 2000$ MW (rating), $P_L = 1000$ MW (nominal loading), $f = 60$ Hz, $B_1 = B2 = 0.045$ p.u. MW/Hz; $R_1 = R_2 = 2.4$ Hz/p.u.; $T_{G1} = T_{G2} = 0.08$ s; $T_{T1} = T_{T2} = 0.3$ s; $K_{PS1} = K_{PS2} = 120$ Hz/p.u. MW; $T_{P1} = T_{P2} = 20$ s; $T_{12} = 0.545$ p.u.

Authors' Information
Appala Naidu Karanam received B.Tech. degree in Electrical and Electronics Engineering from Vignan's Institute of Information Technology, Visakhapatnam in 2010. And M.Tech. degree in Power electronics and drives from VIT University, Vellore in 2013. He is currently pursuing Ph.D. degree in Electrical engineering from NIT Raipur, India. His current research interests include Power system control and soft computing techniques.
Binod Shaw received Ph.D. degree in electrical engineering from the Indian Institute of Technology (ISM), Dhanbad, Jharkhand, India. He is currently working as an Assistant Professor with the Department of Electrical Engineering, National Institute of Technology, Raipur, India. His research interest includes power system control, optimization techniques, renewable energy and application of AI in RES.

References
1. Kothari, M. L., Nanda, J., Kothari, D. P., & Das, D. (1989). Discrete-mode automatic generation control of a two-area reheat thermal system with new area control error. *IEEE Transactions on Power Systems, 4*(2), 730–738.
2. Kumar, P., & Kothari, D. P. (2005). Recent philosophies of automatic generation control strategies in power systems. *IEEE Transactions on Power Systems, 20*(1), 346–357.
3. Rahman, A., Saikia, L. C., & Sinha, N. (2017). Automatic generation control of an interconnected two-area hybrid thermal system considering dish-stirling solar thermal and wind turbine system. *Renewable Energy, 105*, 41–54.
4. Ibraheem, R., Niazi, K. R., & Sharma, G. (2015). Study on dynamic participation of wind turbines in automatic generation control of power systems. *Electric Power Components and Systems, 43*(1), 44–55.
5. Hasanien, H. M., & El-Fergany, A. A. (2017). Symbiotic organisms search algorithm for automatic generation control of interconnected power systems including wind farms. *IET Generation, Transmission and Distribution, 11*(7), 1692–1700.
6. Saikia, L. C., Nanda, J., & Mishra, S. (2011). Performance comparison of several classical controllers in AGC for multi-area interconnected thermal system. *International Journal of Electrical Power and Energy Systems, 33*(3), 394–401.
7. Gorle, P. K., Srinu Naik, R., & Prasad, C. D. (2021). Application of the PI-PD cascade control scheme in AGC of a deregulated power system with PV in the presence of communication delay. *International Journal of Ambient Energy, 52*, 1–12.
8. Dash, P., Saikia, L. C., & Sinha, N. (2015). Automatic generation control of multi area thermal system using Bat algorithm optimized PD-PID cascade controller. *International Journal of Electrical Power and Energy Systems, 68*, 364–372.
9. Patan, M. K., Raja, K., Azaharahmed, M., Prasad, C. D., & Ganeshan, P. (2021). Influence of primary regulation on frequency control of an isolated microgrid equipped with crow search algorithm tuned classical controllers. *Journal of Electrical Engineering and Technology, 16*(2), 681–695.
10. Araki, M., & Taguchi, H. (2003). Two-degree-of-freedom PID controllers. *International Journal of Control, Automation, and Systems, 1*(4), 401–411.

11. Sahu, R. K., Panda, S., Rout, U. K., & Sahoo, D. K. (2016). Teaching learning based optimization algorithm for automatic generation control of power system using 2-DOF PID controller. *International Journal of Electrical Power and Energy Systems, 77*, 287–301.

12. Zhao, X., Lin, Z., Fu, B., He, L., & Fang, N. (2018). Research on automatic generation control with wind power participation based on predictive optimal 2-degree-of-freedom PID strategy for multi-area interconnected power system. *Energies, 11*(12), 3325.

13. Dash, P., Saikia, L. C., & Sinha, N. (2014). Comparison of performances of several Cuckoo search algorithm based 2DOF controllers in AGC of multi-area thermal system. *International Journal of Electrical Power and Energy Systems, 55*, 429–436.

14. Debbarma, S., Saikia, L. C., & Sinha, N. (2014). Automatic generation control using two degree of freedom fractional order PID controller. *International Journal of Electrical Power and Energy Systems, 58*, 120–129.

15. Nayak, J. R., Shaw, B., Sahu, B. K., & Naidu, K. A. (2021). Application of optimized adaptive crow search algorithm based two degree of freedom optimal fuzzy PID controller for AGC system. *Engineering Science and Technology, an International Journal*.

16. Askarzadeh, A. (2016). A novel metaheuristic method for solving constrained engineering optimization problems: Crow search algorithm. *Computers and Structures, 169*, 1–12.

17. Bevrani, H., Feizi, M. R., & Ataee, S. (2015). Robust frequency control in an islanded microgrid: H∞ and μ-Synthesis approaches. *IEEE Transactions on Smart Grid, 7*(2), 706–717.

18. Pan, I., & Das, S. (2014). Kriging based surrogate modeling for fractional order control of microgrids. *IEEE Transactions on Smart grid, 6*(1), 36–44.

19. Hasanien, H. M. (2018). Whale optimisation algorithm for automatic generation control of interconnected modern power systems including renewable energy sources. *IET Generation, Transmission and Distribution, 12*(3), 607–614.